A Revolutionary Framework to Enable High-Fidelity Multiscale Modeling

Su Tian, Bo Peng, Ning Liu, Wenbin Yu

Composites Manufacturing and Simulation Center

Purdue University

Abstract*: The present work provides a new way to carry out multiscale modeling. This method is based on the Mechanics of Structure Genome, a recently developed theory, which can predict effective properties from a Structure Genome, defined as the smallest mathematical building block of the structure, and local strains and stresses from global response at the structure level. A custom toolset is developed to connect the multiscale modeling code to Abaqus/CAE, utilizing its pre- and post-processing capabilities of creating model, meshing and visualization. Three examples, including beam, plate and 3D solid structures, are presented.*

Keywords*: Multiscale, Abaqus, Mechanics of Structure Genome, SwiftComp*

1 Introduction

The primary challenge in high fidelity multi-scale modeling has been the need for a framework to couple traditional finite element methods to multiple scales while achieving necessary efficiencies. An Abaqus custom toolset is developed to enable efficient high-fidelity multiscale modeling using the conventional elements of Abaqus. The Mechanics of Structure Genome (MSG), a recently discovered multiscale modeling framework based on the concept of Structure Genome (SG) provides the foundation for this new approach (Yu, 2016). SG is defined as the smallest mathematical building block of a given structural system. MSG uses the principle of minimum information loss to perform a multiscale constitutive modeling to minimize the loss of information between the original heterogeneous body and the equivalent homogenized body. Depending on the geometric characteristic of the structure, MSG can compute effective properties for beams, plates, shells, and 3D solids.

As shown in Figure 1, the toolset exploits the versatile pre-processing capabilities of Abaqus/CAE to create a finite element mesh of the SG to obtain effective structural properties which are then used as inputs for macroscopic analyses using Abaqus elements. The macroscopic behavior can be further used as inputs to predict the local stress, strain and displacement fields within the SG, which are then visualized using the post-processing capabilities of Abaqus/CAE. Several examples are presented including simulation of composites helicopter and wind turbine blades, buckling of stiffened composite structures, multiscale modeling of interlock textile composites to demonstrate the benefits of the MSG approach. The Abaqus custom toolset can be downloaded from cdmHUB at https://cdmhub.org/resources/1134.

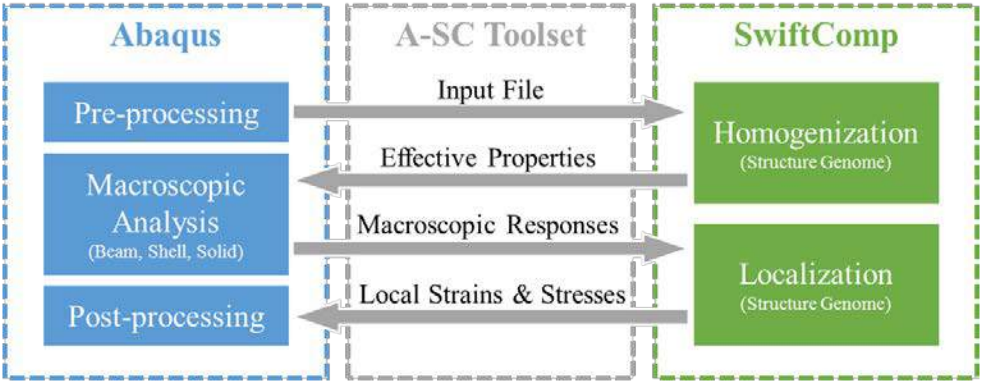

Figure 1. Framework of multiscale modeling based on the integration of Abaqus and SwiftComp.

2 Examples

2.1 Composite Helicopter and Wind Turbine Blade

Helicopter rotor blade and wind turbine blade are both slender structures, which means that the sizes of the two dimensions in the cross-sectional plane are much less than the length along the blade axis. Thus, the blade can be treated as a beam structure and use the cross-section as the SG to capture all behaviors of the structure. For a beam with uniform cross-sections, only one SG is needed to calculate the complete stiffness matrix. A real blade usually has a varying cross-section. Many sections as needed can be cut along the beam axis as SGs to approximate the real blade structure as a beam.

In this example, an airfoil-shaped cross-section is used to represent typical helicopter rotor or wind turbine blades. This typical blade is assumed having uniform cross-sections, which means only one cross-section is used as the SG to calculate the beam stiffness matrix, shown in Figure 2. The detailed sectional geometry is shown in Figure 3. As shown in the figure, there are four different layups for both low pressure surface and high pressure surface, two webs and one area filled with foam. The chord length is 1.9 in., and the reference point is 25% of the chord length away from the leading edge. Materials used in this example are listed in Table 1. All required data are stored in four xml files and the model is created by importing these data using the Abaqus-SwiftComp Toolset. Then the toolset will generate an input file and SwiftComp will compute the effective properties, which are listed in Table 2, where diagonal entries from upper left to lower right are EA, GJ, EIflap and EIedge, respectively.

Next, the cross-sectional stiffness will be used to do a macroscopic analysis of a beam model. The total length of the structure is 20 in. One end (x_1=0) is fixed and the other end (x_1=20 in) is applied a concentrated force load of 1000 lb along the positive x_3 direction. At this step, since the beam element in Abaqus cannot take all entries in the stiffness matrix to capture the response, another code named GEBT (Geometrically Exact Beam Theory) is used as the analysis tool. After getting the results of macroscopic analysis, localization is carried out for a cross-section at the middle span (x_1=10 in) of the blade. Finally, recovered local strains and stresses are imported back into

Abaqus/CAE for visualization. Several contour plots showing 3D stress distributions over the cross section are shown in Figure 4.

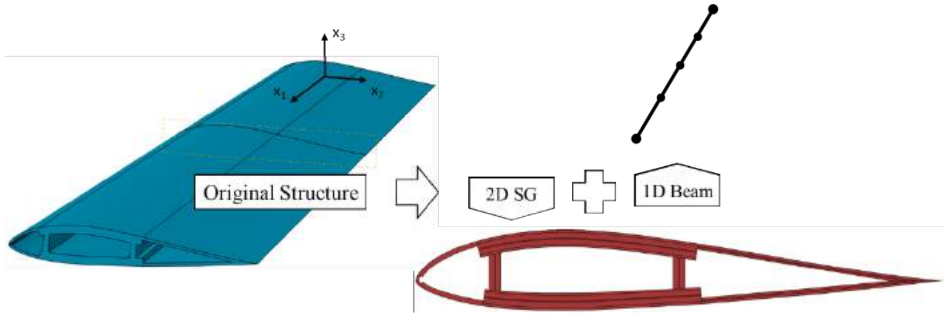

Figure 2. Decomposition of the original structure into a 2D Structure Genome and a 1D macroscopic beam model.

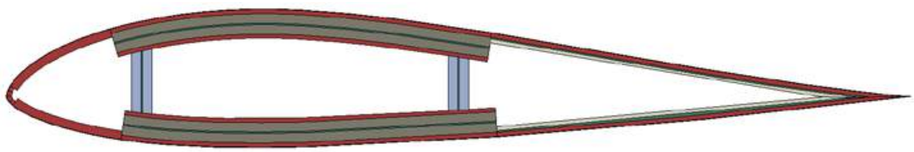

Figure 3. A cross-section is chosen as the Structure Genome for homogenization.

Table 1. Properties of materials used in the composite blade example.

	E1	E2	E3	G12	G13	G23	v12	v13	v23
	psi								
uni-directional FRP	37.0E+09	9.0E+09	9.0E+09	4.0E+09	4.0E+09	4.0E+09	0.28	0.28	0.28
double-bias FRP	10.3E+09	10.3E+09	10.3E+09	8.0E+09	8.0E+09	8.0E+09	0.3	0.3	0.3
Gelcoat	10.0	10.0	10.0	1.0	1.0	1.0	0.3	0.3	0.3
Nexus	10.3E+09	10.3E+09	10.3E+09	8.0E+09	8.0E+09	8.0E+09	0.3	0.3	0.3
Balsa	10.0E+06	10.0E+06	10.0E+06	0.2E+06	0.2E+06	0.2E+06	0.3	0.3	0.3
	E(psi)	**v**							
Foam	72.4E+09	0.3							

Table 2. Effective properties of the blade.

2.391776E+09	-3.364331E+07	6.977756E+07	-5.530447E+08
-3.364331E+07	2.160163E+07	-1.412434E+06	2.360207E+06
6.977756E+07	-1.412434E+06	2.093010E+07	-9.036410E+06
-5.530447E+08	2.360207E+06	-9.036410E+06	4.795876E+08

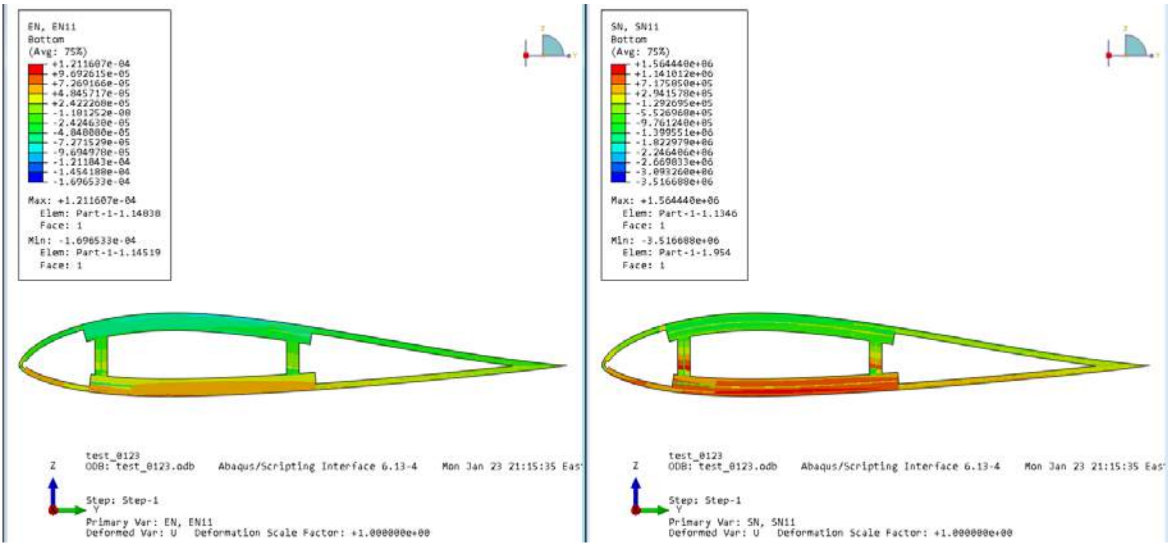

Figure 4. Visualization of selected local strains and stresses of the cross-section at the middle span.

2.2 Buckling of Stiffened Composite Structures

In this example, the authors built a double-sided orthogonal stiffened panel (DOSP). SG of the panel is 0.7 m long and 0.28 m wide where orthogrid is stiffened on both sides, as shown in Figure 5. It is repeated nine times along both directions to build the panels (6.3 m long and 2.52 m wide). The stiffeners are 0.003 m wide and 0.02 m tall. Skin thickness is 0.002 m. A metallic material is used, with properties of E=72 GPa and ν=0.33. Uniaxial compressive loads are applied along longitudinal at the shorter edge, and all the edges are simply supported meaning that their out-of-plane deflection is constrained.

In MSG-based approach, constitutive relations, i.e., ABD matrices are obtained by carrying out the constitutive modeling over the SG in SwiftComp at first. The results are reported in Table 3. Then Abaqus carries out the linearized buckling analysis using the constitutive relations defined as the general shell stiffness of 2D shell elements (S8R5). Detailed FEA is performed using 3D solid elements (C3D20R) in Abaqus. The lowest six buckling loads and mode shapes of MSG and detailed FEA are reported in Figure 6. Each pair has a buckling load in Newton under its corresponding buckling mode shape. Solutions of the MSG-based approach are referred as "MSG" whereas solutions of the detailed FEA are referred as "3D FEA". Comparing with the results of 3D FEA, the MSG-based approach predicts the same buckling mode shapes, and the errors in the prediction of buckling loads are less than 4%. Highest error is observed to be 3.29% in mode 6, whose buckling wavelength is longer but close to the distance between stiffeners. Current MSG-based approach is based on a premise that buckling wavelength is larger than the distance between stiffeners. The approach will lose accuracy particularly when buckling wavelength is close to or shorter than the distance between stiffeners.

The investigation of post-buckling behavior using the MSG-based approach is presented next. The nonlinear post-buckling is solved using Abaqus's Static Riks method. Imperfection factors are introduced. First three buckling modes are used to construct the imperfection. The imperfection size, i.e., imperfection scaling factors are 2.0E-04, 1.0E-04 and 0.5E-04, which are associated with the first three modes, respectively.

Convergence study is carried out to decide the stopping criterion for the iteration. Results are presented with 400 steps, minimum arc length of 1.0E-08 and maximum arc length of 0.1. Since current work studies the elastic buckling behavior without considering material yielding, structural collapse is not studied.

Load-displacement curves of MSG-based approach and 3D FEA are presented in Figure 7. Vertical coordinate represents the normalized axial load with P_{cr} as the critical buckling load predicted in the linear buckling step. Axial shortening is measured at the geometric center of the cross-section. It is seen that stiffened panels are still stable in post-buckling regime but have reduced stiffness in this example. Agreement between MSG-based approach and 3D FEA is observed to be excellent. Element numbers and computing time of both approaches to carry out the post-buckling analysis are reported in Table 4. It can be seen that the MSG-based approach requires less computational efforts, yet achieves same level of accuracy with 3D FEA.

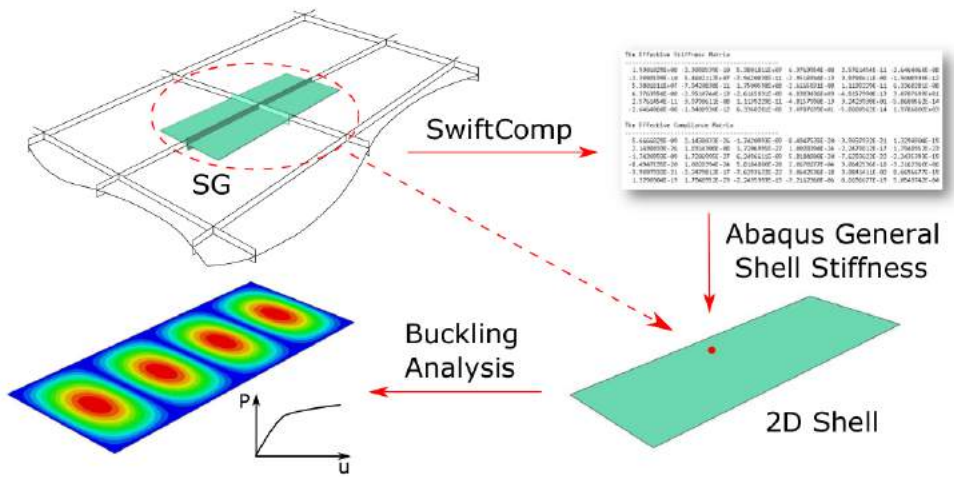

Figure 5. Buckling analysis workflow using the MSG-based approach.

Table 3. Constitutive relations (ABD matrix) of DOSP with the metallic material.

1.9301E+08	5.3802E+07	0	0	0	0
5.3802E+07	1.7501E+08	0	0	0	0
0	0	5.4602E+07	0	0	0
0	0	0	4.8383E+03	30.7877	0
0	0	0	30.7877	1.9787E+03	0
0	0	0	0	0	32.4239

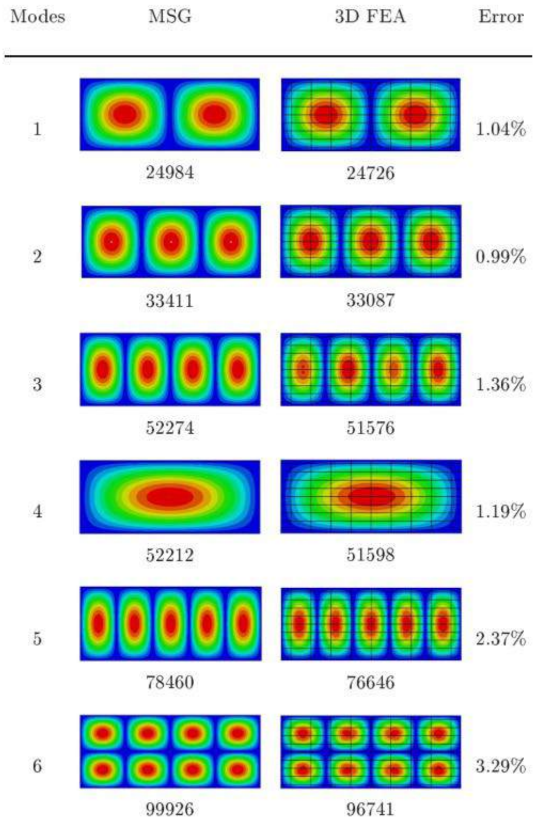

Figure 6. Buckling loads (N) and mode shapes.

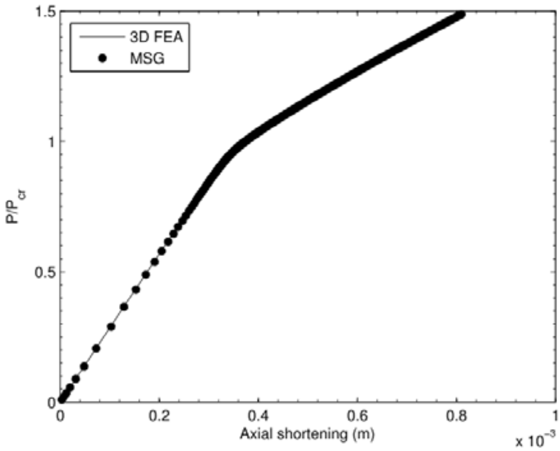

Figure 7. DOSP with the metallic material: force-displacement curve.

Table 4. Number of elements and computing time of the post-buckling analysis by the MSG-based approach and the 3D FEA, respectively.

	MSG	3D FEA
Number of elements	1575 (shell)	645408 (brick)
Computing time	17 min (1 CPU)	3 days 18 hrs (32 CPUs)

2.3 Interlock Textile Composites

The 3D orthogonal interlock textile composite plate is simulated in three ways as shown in Figure 8. In the two multiscale simulations, the homogenization and localization are performed with SwiftComp and Abaqus RVE analysis (Solid-to-shell) respectively, and the macroscopic plate analysis is conducted using STRI3 elements in Abaqus. The plate is also analyzed by direct 3D FEA in Abaqus.

The geometry details of the SG are shown in Figure 9. It is noted that there is a horizontal portion of z-tow in the upper part of the SG. The material properties of constituents are listed in Table 5. As shown in Figure 10, the plate is constrained at the left side, and transversely loaded at the right side by a uniform traction along x_3.

In the multiscale simulation, first the effective plate stiffness matrices are generated by SwiftComp and Abaqus RVE plugin respectively. As shown in Table 6 and Table 7, the obtained plate stiffness matrices are very close, of which the maximum difference of the corresponding components is 0.7%. Then the global sectional strains and curvatures are obtained by implementing the effective plate stiffness matrices in the macro plate model.

Localization analyses are performed at the SG located at (37.5, 7.5) of the plate using SwiftComp and Abaqus RVE plugin respectively, where the global sectional strains and curvatures are presented in Table 8. The stress distributions on the sampling paths Line A, B and C through the thickness shown in Figure 10 are investigated. The macro coordinates (x_1, x_2) of the three paths Line A, B and C are (37.5, -1.5), (37.5, 0.0) and (39.0, -3.0). The stress component σ_{11} at these three paths is compared in Figure 11. Only σ_{11} is presented because the other components are closing to zero subjected to the loading considered. Good agreement of the stress distribution with the 3D direct FEA results shows the effectiveness of the multiscale simulation tools of both SwiftComp and Abaqus RVE plugin.

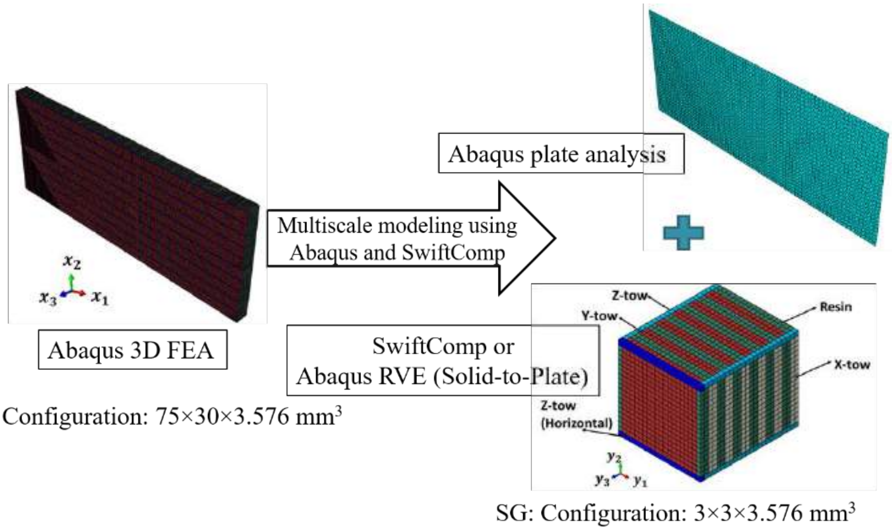

Figure 8. Modeling interlock textile composite plate in three ways: multiscale simulation using SwiftComp/Abaqus RVE plugin and plate analysis; direct FEA in Abaqus.

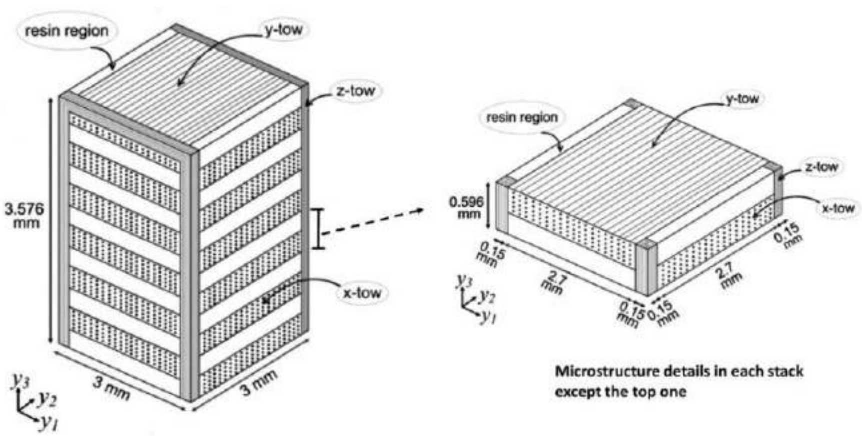

Figure 9. SG of the orthogonal interlock composites. (Nasution, 2014)

Table 5. Material properties of the orthogonal interlock composites. (Nasution, 2014)

Properties	X-tow	Y-tow	Z-tow	Resin
E_1 (Gpa)	122.55	7.13	4.96	3.4
E_2 (Gpa)	7.13	122.55	4.96	3.4
E_3 (Gpa)	7.13	7.13	148.7	3.4
G_{12} (Gpa)	3.25	3.25	2.45	1.26
G_{13} (Gpa)	3.25	2.53	3.21	1.26
G_{23} (Gpa)	2.53	3.25	3.21	1.26
v_{12}	0.263	0.015	0.476	0.35
v_{31}	0.015	0.414	0.335	0.35
v_{23}	0.414	0.263	0.011	0.35

Table 6. Plate stiffness matrix generated by SwiftComp.

213339	6857	0	357273	12181	0
6857	204572	0	12231	382208	0
0	0	10635	0	0	19019
357273	12231	0	826711	28866	0
12181	382208	0	28866	918074	0
0	0	19019	0	0	45326

Table 7. Plate stiffness matrix generated by Abaqus RVE plugin.

213330	6858	0	357260	12189	0
6858	204310	0	12224	381350	0
0	0	10634	0	0	19018
357260	12224	0	826490	28677	0
12189	381350	0	28677	915100	0
0	0	19018	0	0	45324

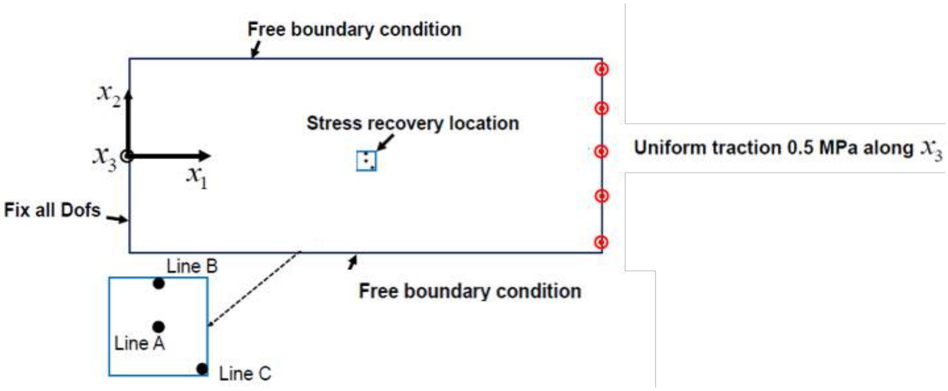

Figure 10. Boundary conditions of the composite plate and the location of the localization analysis.

Table 8. Global section strains and curvatures at the interested location of the plate.

	ε_{11}(SE1)	ε_{22} (SE2)	γ_{12} (SE3)	K_{22} (SK2)	K_{11} (SK1)	K_{12} (SK3)
Abaqus RVE	4.9216E-04	-1.8233E-05	-1.0151E-07	1.0340E-05	-2.9392E-04	-6.6205E-10
SwiftComp	4.9206E-04	-1.8614E-05	-1.5283E-06	1.0544E-05	-2.9384E-04	8.3356E-07
Difference (%)	0.02	-2.05	-	-1.94	0.03	-

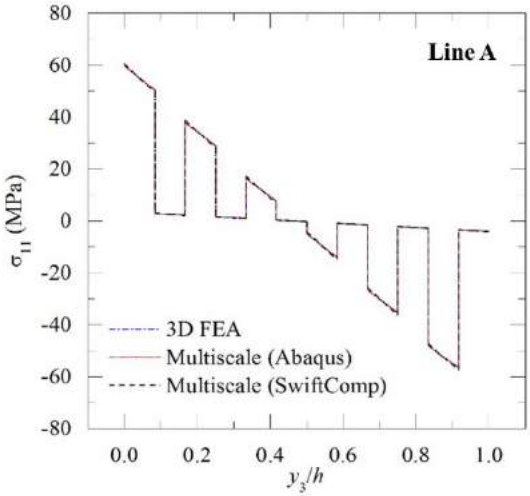

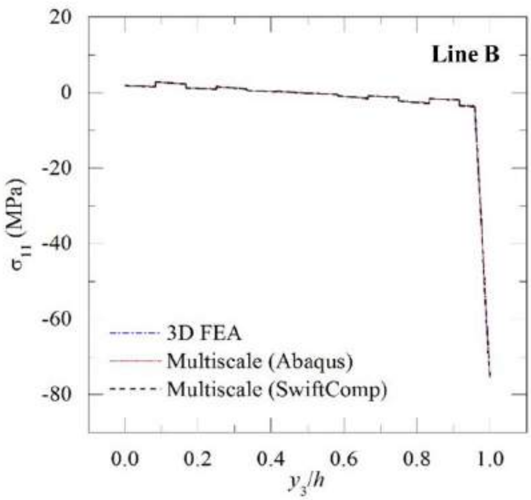

Figure 11. Comparison of the stress distribution at Line A and B. The horizontal axis is the normalized location in the thickness direction, of which h is the total thickness of the plate.

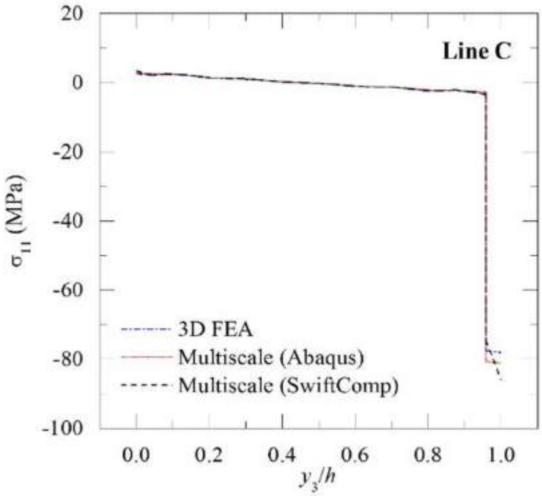

Figure 11. Comparison of the stress distribution at Line C. The horizontal axis is the normalized location in the thickness direction, of which *h* is the total thickness of the plate.

3 Conclusions

A complete framework for high-fidelity modeling is presented in this work. This method requires users to identify the smallest building block of the structure and decompose the original model into a detailed Structure Genome and a simple macroscopic model. This framework is based on the Mechanics of Structure Genome, which is built on the Principle of Minimum Information Loss. The theory is realized by SwiftComp and a custom toolset is developed to integrate Abaqus and SwiftComp. The three examples, a beam-like structure, a plate-like structure and a solid structure, show that the framework can help users to build the Structure Genome easily and carry out the modeling accurately and quickly.

4 References

1. Micromechanics Plugin For Abaqus/CAE Version 1.0 (Manual), Dassault Systèmes.
2. Nasution, M.R.E., Watanabe, N., Kondo, A. and Yudhanto, A., 2014. “A novel asymptotic expansion homogenization analysis for 3-D composite with relieved periodicity in the thickness direction,” Composites Science and Technology, 97, pp.63-73.2014.
3. Yu, W.: “A Unified Theory for Constitutive Modeling of Composites,” *Journal of Mechanics of Materials and Structures*, vol. 11, no. 4, 2016, pp. 379-411.